Pressure filtration properties of sludge generated in the electrochemical treatment of mining waters

Gafiullina Anastasia, Mamelkina Maria, Vehmaanperä Paula, Kinnarinen Teemu, Häkkinen Antti

DOI: 10.1016/j.watres.2020.115922

Pressure filtration properties of sludge generated in the electrochemical treatment of mining waters

Anastasia Gafiullina*, Paula Vehmaanperä, Maria Mamelkina,

Teemu Kinnarinen, Antti Häkkinen

Department of Separation Science, LUT School of Engineering Science,

Lappeenranta-Lahti University of Technology, Yliopistonkatu 34, FI-53850

Lappeenranta, Finland

E-mail: anastasia.gafiullina@lut.fi

Keywords: electrochemical water treatment, electrocoagulation, mining water, pressure filtration, cake resistance, filter aids.

ABSTRACT

In this study, batch electrocoagulation (EC) experiments were performed with synthetic mining water in various conditions in a laboratory-scale 1L reactor. The process was scaled up and the selected results were verified with both synthetic and real mining water in a 70 L reactor. The generated solids were characterized by XRD, SEM, and a laser diffraction particle size analyzer. After preconcentration by settling and decantation, the EC solids were separated by constant pressure filtration at 2–6 bar. In order to improve the separation, various filter aids were used in body-feed and precoat modes.

The results show that the overall removal efficiency was the highest with consumable electrode pairs such as Fe/Fe, Al/Al and Fe/Al, and the highest treatment efficiency was achieved with Fe/Al electrodes where 100/100% of the nitrate and 96/87% of the sulfate were removed in small/large-scale experiments. Depending on the dissolved electrode material, different solid species were formed: crystalline primary particles with a minor degree of agglomeration were observed in Fe/Fe slurry, whereas aluminium-containing solids (Al/Al and Fe/Al) were mainly amorphous agglomerates. High values of average specific cake resistances (α_{av} = $2 \cdot 10^{12}$ - $4 \cdot 10^{13}$), average porosities (> 90%) and moisture contents (> 68wt%) of filter cakes were obtained for all filtered samples. The highest values of the above-mentioned cake characteristics were observed for aluminium-based solids, which might be explained by its highly amorphous structure. The application of filter aids improved the filterability of the sludges by reducing the average specific cake resistance by as much as 95–96% in the body-feed mode and by 84% in the precoat mode.

1. Introduction

The mining industry is known as a source of huge volumes of solid waste. On average, 1,750 and 2,000 megatons (Mt) of solid mining waste is annually produced in Australia and in the USA respectively, and more than 4,700 Mt of mining waste is stored in EU countries (Lottermoser, 2010). Along with waste generation, the mining industry produces a huge amount of mining water that is used in many stages, including: core processes such as beneficiation, hydrometallurgical

extraction, and secondary operations, i.e. dust suppression (Lottermoser, 2010). The amount of pure consumed water can be substantially reduced by recycling purified mining water. Proper treatment is also required prior to water discharge, because polluted mining effluent may cause contamination of surface and ground water (Lottermoser, 2010), severe effects on aquatic life due to metal toxicity (Seal et al., 2008; Simate and Ndlovu, 2014), degradation of soils (Simate and Ndlovu, 2014) and irrigated crops (Dolenec et al., 2007), and may prevent downstream water consumption by human beings (Cidu and Fanfani 2002; Sarmiento et al., 2009).

The techniques used for mining water treatment can be generally divided into active processes characterized by the continuous addition of chemicals and active maintenance (Lottermoser, 2010); and passive systems where the naturally occurring biochemical processes are used for water purification (Ben Ali et al., 2019). Corresponding mechanisms of the treatment, targeted pollutants, limitations and other details for each particular technique can be found elsewhere (Cui et al., 2006; Younger et al., 2002).

Conventional active and passive techniques are effective in the treatment of metal cations and suspended solids, but generally they do not achieve the desired removal efficiency for other mining water constituents. Among these, a special concern is caused by the presence of metals of high toxicity (As, Cd, Hg, Pb) (Duruibe et al., 2007), nitrates, cyanides (Hassani et al., 2011, Mamelkina et al., 2020) and sulfate (Mamelkina et al., 2017). Advanced treatment technologies can be considered as an alternative approach to deal with these pollutants.

Electrocoagulation (EC) is an electrochemical treatment and is an emerging purification technique for the simultaneous removal of various substances present in mining waste waters. Descriptions of the mechanism of EC treatment can be found elsewhere (Emamjomeh and Sivakumar, 2009a; Mollah et al., 2001; Sahu et al., 2014). EC takes advantage of electroflocculation, electrosorption, electrooxidation, electroreduction, and electroflotation, which occur between the electrodes of a reactor at the same time as the EC proceeds and thus enables wide range of pollutants to be treated with a high degree of performance (Kabdaşlı et al., 2012; Liu et al. 2017). EC provides additional advantages, such as reactor simplicity, ease of operation, and its chemical-free nature (Chen, 2004; Holt et al., 2002; Mollah et al., 2001). By nature, sludge formed by EC is relatively low in amount, readily settleable, and easy to dewater (Mollah et al., 2001).

In terms of scale-up, electrocoagulation is defined as difficult but quantifiable or very difficult and rarely quantifiable technique (Harmsen, 2013). The scale-up is hindered by the various mechanisms involved in contaminants removal and solids generation. Among the most significant scale-up parameters are the ratio of electrode surface area to volume of a treated solution, current density, electrical charge, flow regime, reactor configuration and geometry (Zolotukhin et al., 1989, Mamelkina et al., 2017). In this paper, the current density and the reactor geometry have been assessed as possible scale-up parameters for an EC process.

In EC, the dissolution of sacrificial electrodes releases metal cations, based on Faraday's law. The reactions between the released metal cations and those present in the mining water with OH groups stemming from water electrolysis form insoluble metal hydroxides and metal oxides. As a result, the formed oxides and hydroxide can adsorb some pollutants such as sulfate (Murugananthan et al. 2004), fluoride (Emamjomeh et al., 2011; Zhu et al., 2007), and phosphate (Lacasa et al., 2011a), which in turn settle as solid matter.

To achieve the full use of EC in the treatment of mining water, there is a need to investigate a suitable solid-liquid separation technique for the separation of such solid matter, because improper separation leads to the production of low-quality filtrate and solid waste with a high moisture content. The application of pressure cake filtration is widespread in mineral processing industries, due to its ease of operation, high capacity, and the minimization of waste production (Rushton et al., 2000; Townsend, 2003). Using an appropriate filter medium with suitable process parameters, the separation and energy efficiency and the capacity of a cake filtration process can be significantly improved (Svarovsky, 2000).

The average specific cake resistance is regarded as an indicator of the ease of cake filtration. A high average specific cake resistance may make it necessary to pretreat the slurry prior to filtration. The pretreatment can be achieved, e.g., by introducing chemicals such as flocculants, solvents, or surfactants (Wakeman, 2007), or by applying physical methods such as heating, cooling, elutriation and thickening (Tarleton and Wakeman, 2007). The addition of filter aids (FAs) is considered an alternative technique to enhance the performance of filtration (Ripperger et al., 2012). FAs can be precoated onto the surface of the filter medium or introduced as an additive in slurry (body feed). The former approach improves filtrate clarity, and the latter primarily reduces specific cake resistance by changing the cake properties such as porosity, rigidity, and tortuosity (Carman, 1938; Kinnarinen et al., 2013). The optimization of the FA dosage is of critical importance (Svarovsky, 2000). As a rule of thumb, the FA dosage should be on the order of the solids content in the slurry, however the dosage should be defined experimentally as it is highly case dependent (Carman, 1938).

The present study is the first in which an enhanced mining water purification process is investigated considering the removal of coagulated matter using cake filtration. The aims is to form a thick cake, which itself is responsible for the retention of solids, instead of filtration through a microfiltration membrane (pore size = 0.1 - 1 μm), in which the membrane is the primary separation medium and the formation of a thick cake is avoided. The purification process introduced in this paper includes electrochemical water treatment and a filtration stage, which are evaluated referring to the characteristics of the produced solids.

2. Materials and methods

2.1. Materials

Specification of the treated water solutions and main characteristics of the used electrodes and filter aids are described in the section.

2.1.1. Mining waters

Both synthetic water solutions and real mining water were electrochemically treated. Synthetic mining water was prepared by means of dissolving sodium nitrate (> 99.2%, Eurolab Oy), ammonium chloride (> 99.5%, Mallinckrodt Baker B.V.), sodium chloride (> 99.5%, BDH Prolabo, VWR Chemicals) and sodium sulphates (> 99.0%, EMD Millipore Corporation) in pure water (Millipore). The contaminants of interest were selected based on the current limits for these constituents in Nordic countries (Wahlström et al., 2017) and increasing interest from mining companies to develop suitable technologies to remove the contaminants. The removal of metals from mining water by EC has already been extensively studied, whereas the removal of nitrate – whether being tested in general – was not investigated for mining water. Thus, sulfate and nitrate

anions have been chosen as targeted species. The initial concentrations of ionic species to be present in synthetic solution (Table I) were defined based on the average values of these constituents in real mining water provided by several Nordic mines. The initial pH was adjusted to pH 3, 7, and 11 by using 0.1M NaOH or 0.1M HCl.

Real mining water was collected from the Orivesi mine, Pirkanmaa region, Finland, and was stored in a fridge at a temperature of 4 °C. The concentrations of the species of interest for the study detected in the mining water are presented in Table I. The initial pH was adjusted to pH 3 by using 0.1M HCl.

Table I. Initial concentrations of the target species present in synthetic and real mining water.

Species	Unit	Synthetic solution	Real mining water
NO_3^-	mg/L	10	255.14
SO_4^{2-}	mg/L	1000	2561.32
NH_4^+	mg/L	15	0
Al	µg/L	0	404.03
Co	µg/L	0	23.23
Cu	µg/L	0	38.65
Fe	µg/L	0	119.12
Ni	µg/L	0	12.96
Zn	µg/L	0	71.41

2.1.2. Electrodes

The following electrode pairs (anode/cathode) with dimensions of 60×70×2 mm and a total anode area of 168 cm^2 were used in laboratory-scale experiments: Fe/Fe, Al/Al, Fe/Al, Al/Fe, Fe/C, Al/C, Fe/Ti, Al/Ti, Ti/Ti, C/C, Ti/C, C/Ti. Pilot-scale tests were performed using Fe/Fe, Al/Al and Fe/Al electrode combinations; the dimensions of these electrodes were 300×300×5 mm resulting in a total anode area of 3,600 cm^2.

2.1.3. Filter aids

Four different filter aids—diatomaceous earth (DE) (D_{50} = 18.1 µm), rice hull ash "MaxFlo Grade 4" (D_{50} = 46.7 µm) (RHA Grade 4), rice hull ash "MaxFlo X+100" (D_{50} = 69.1 µm) (RHA X+100), and milled cardboard (D_{50} = 220.3 µm)—were chosen based on a previous study by Kinnarinen et al. (2013), where also data on the properties of the materials can be found

2.2. Methods

Experimental set-up and test procedures are described below and summarized in Table II.

2.2.1. Electrochemical water treatment

The electrochemical treatment of synthetic mining water was performed in a batch mode in a laboratory-scale reactor (V = 1L) and in a pilot-scale reactor (V = 70L), both made from plexiglass. The EC treatment of real mining water was performed in a 70L reactor. At the scale-up stage, to

guarantee the most appropriate sizing of the equipment and ensure geometrical similarity of the reactors, the dimensions of 1L reactor were enlarged 4 times resulting in the possible treatment volume of 70L. The equipment set-up (Fig. 1) was similar in both laboratory- and pilot-scale experiments.

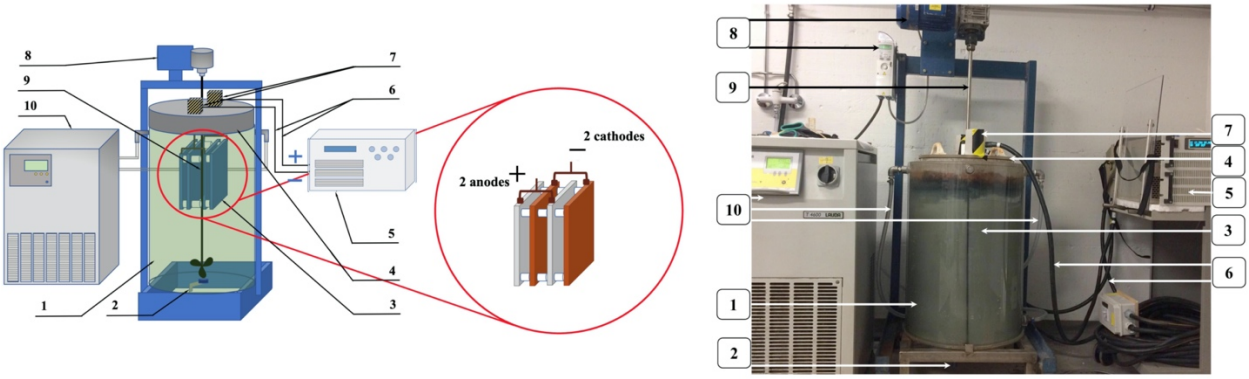

Fig. 1. A schematic view (left) and a picture (right) of pilot-scale experimental set-up used to perform electrocoagulation: (1) reactor tank, (2) bottom valve, (3) electrodes assembly, (4) reactor cover, (5) power supply system, (6) cables, (7) high voltage protection, (8) mixing unit with a frequency converter, (9) stirrer, (10) cooling system with hosepipes.

Two pairs of electrodes (two anodes/two cathodes) were connected in a monopolar arrangement and submerged in a reactor filled with a solution to treat. Prior to EC, the pH was adjusted to 3, 7, or 11 in the small-scale experiments, whereas the initial pH was 3 in the larger-scale tests. The treatment started when a current was applied to the system and lasted for 5 hours. To minimize the effect of electrodes passivation, the polarity of the electrodes was changed every hour in the experiments with Fe/Fe, Al/Al, Ti/Ti and C/C pairs. Samples were taken from the solution after 30 min, and after 1, 2, 3 and 5 hours of treatment to monitor the removal of nitrate, sulfate, chloride, ammonia and total nitrogen from the solution, and for characterization of the generated solid matter.

2.2.2. Pressure filtration

To produce the feed sludge for the pressure filtration experiments, the obtained EC sludges were left to settle for 48 hours. Only the thickened bottom layer of each of obtained sludge was collected for the experiments. Pressure filtration experiments were performed with a Nutsche filter (Fig. 2) that consisted of a 350 mL cylindrical filter chamber (⌀ = 52 mm). T120 cellulose/perlite filter medium discs (Pall Corporation) with a retention range within 2.5 – 4.5 µm and permeability of 213 L/(m^2·min·bar) (PALL Data Sheet, 2011) were used in all pressure filtration experiments.

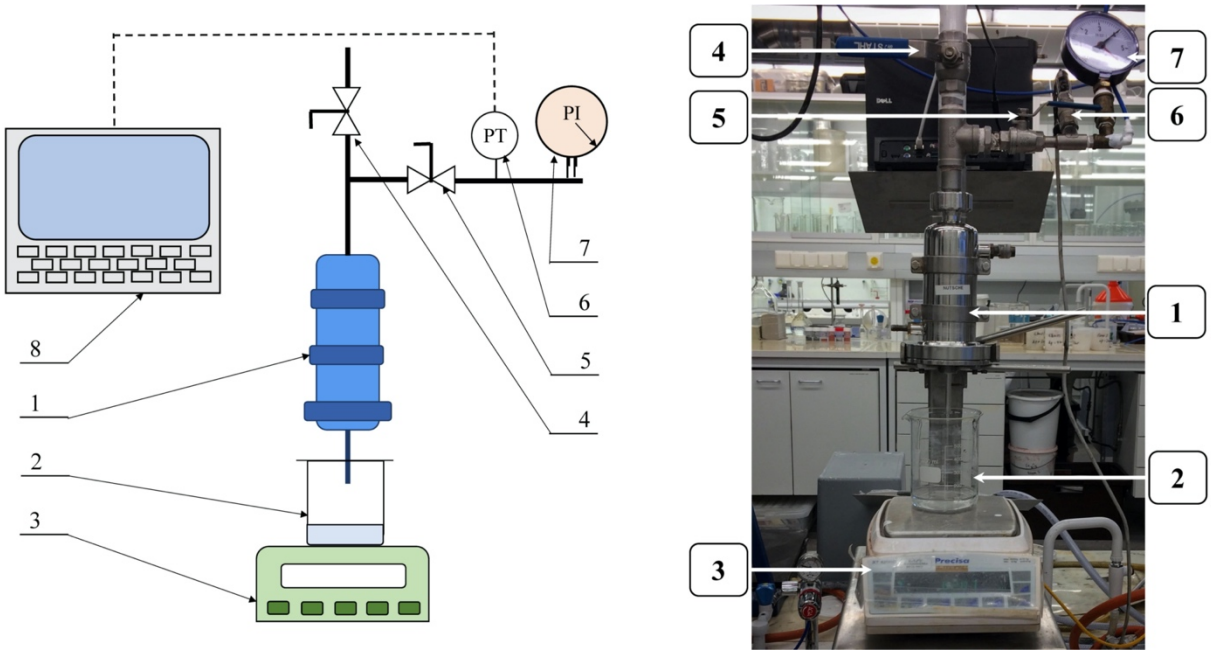

Fig. 2. A schematic view (left) and a picture (right) of experimental set-up used to perform pressure cake filtration: (1) filter chamber, (2) beaker for filtrate collection, (3) scale, (4) slurry valve, (5) gas valve, (6) pressure transmitter, (7) pressure gauge, (8) computer with the LabVIEW system.

Prior to each experiment, the disc was thoroughly wetted with deionized water. Different sludge volumes (100, 200 and 300 mL) were tested and the applied pressure differences were 2, 4 and 6 bar. An automatic data collection system (LabVIEW by National Instruments, USA) was used to record the mass of the filtrate and the pressure once a second. After each filtration experiment, the filter cake was dried in an oven (24h at 105 °C) in order to determine its moisture content.

2.2.3. Filtration with filter aids

The effect of filter aids (FAs) on the filtration performance was investigated using Fe/Al sludge and both body feed and precoat modes were studied. All the above-mentioned FAs were applied in the precoat tests, while only three materials (diatomite and two rice hull ashes) were used in the body feed tests. Cardboard was found not to be a suitable material for the body feed tests, because it stuck to the walls of the inlet tube when poured into the filter chamber.

To perform pre-coat filtration, the FAs were mixed with pure water at a concentration of 2.05 wt% which was equal to the concentration of solids in the Fe/Al sludge. 100 mL of FA-suspension was filtered with a Nutsche filter under the pressure of 1 bar creating a pre-coated layer on the surface of the filter medium. After that, without any disassembly of the filter, 200 mL of Fe/Al sludge was poured into the chamber and filtration was performed under the pressure of 6 bar.

For testing the body feed mode, FAs were mixed with Fe/Al sludge at the ratios of 0.5:1, 1:1 and 2:1, i.e. the mass of the FAs to the initial solids content of the sludge, and 200 mL of this suspension was filtered at 6 bar. Additionally, the filtration was conducted under the pressure of 2 and 4 bar with the sludge containing FAs at the ratio of 2:1.

2.3. *Analyses*

The concentrations of anions and cations were measured using an ion chromatograph (Metrohm 930 Compact IC Flex) coupled to a conductivity detector. The concentration of total nitrogen (TN) was measured using a total organic compound analyzer (Shimadzu TOC-L/CPH). The pH was measured in-situ at 25° C with a WTW SenTix 22 pH electrode. X-ray diffraction (XRD, Bruker D8 Focus) with CuKα radiation was used to analyze the mineralogical composition of the solid phase. Prior to analysis, the sample was placed in a sample holder and left for 6 h at room temperature to let the liquid evaporate. A scanning electron microscope (SEM, Hitachi SU 3500 with Thermo Scientific, UltraDry SDD EDS) was used to estimate the size range as well as the morphology of the solids. The volumetric particle size distribution was obtained with a laser diffraction particle size analyzer (Mastersizer 3000, Hydro EV unit, Malvern).

Table II. Experimental design (summary).

Operation	Mode	Treated material	
		*Synthetic mining water**	*Real mining water**
Electrochemical treatment (electrocoagulation)	Small-scale reactor (1 L)	**Main studied parameter:** effect of electrode material (anode/cathode): Fe/Fe, Al/Al, Fe/Al, Al/Fe, Fe/C, Al/C, Fe/Ti, Al/Ti, Ti/Ti, C/C, Ti/C, C/Ti. **Varied parameters:** initial solution pH = 3, 7, 11. **Operational conditions:** monopolar electrode arrangements, current density = 17 mA/cm^2, solution stirring at 150 rpm, duration of test run = 5 h. **Determined:** pH and concentration of ionic species.	N/a**
	Pilot-scale (70 L)	**Main studied parameter:** effect of electrode material: Fe/Fe, Al/Al, Fe/Al. **Operational conditions:** same as in 1L reactor tests. **Determined:** pH and concentration of ionic species in the treated solution; PSD, XRD and SEM analyses of the formed solids.	**Main studied parameter:** effect of electrode material: Fe/Fe, Al/Al. **Operational conditions:** same as in 1L reactor tests. **Determined:** pH and concentration of ionic species in the treated solution.
		*Slurries*** generated during EC of synthetic solution*	*Slurries*** generated during EC of real water*
Pressure cake filtration	Nutsche-type filter	**Main studied parameter:** effect of the minerals consisted solid fraction (slurry type) determined by the electrode materials used in EC: Fe/Fe, Al/Al, Fe/Al. **Varied parameters:** operating pressure, Δp, = 2, 4, 6 bar; volume of slurry filtered per batch, V_{sl} = 100, 200, 300 mL. **Determined:** average specific resistance, moisture content, porosity and compressibility of filter cakes.	**Main studied parameter:** slurry type: Fe/Fe, Al/Al. **Varied parameters:** Δp = 2, 4, 6 bar. **Operational conditions:** V_{sl} = 200 mL. **Determined:** average specific resistance, moisture content, porosity and compressibility of filter cakes.
Filter aids assisted	Pre-coat	**Main studied parameter:** effect of filter aid (FA) material: diatomaceous earth, hammer-milled cardboard, RHA X+100, RHA Grade 4.	N/a

		Operational conditions: volume of FA suspension = 100 mL, precoating Δp = 1 bar, V_{sl} = 200 mL, filtration Δp = 6 bar. **Determined:** filtrate recovery, average specific resistance and moisture content of filter cakes.	
	Body feed	**Main studied parameter:** effect of FA material: diatomaceous earth, RHA X+100, RHA Grade 4. **Varied parameters:** FA concentration, wt-%: (25), 50, 100, 200; operating pressure = 2, 4, 6 bar. **Operational conditions:** volume of the filtered sample (slurry mixed with FA) = 200 mL. **Determined:** filtrate recovery, average specific resistance and moisture content of filter cakes.	N/a

* Specifications of synthetic and real mining waters were as shown in Table I for all experiments.
** N/a indicates that no experiments were made.
*** Specifications of the obtained slurries (such as solid content) were as shown in Table IV for all experiments.

4. Calculations

The removal efficiency of the target compounds can be calculated with Eq. (1):

$$RE = \frac{c_0 - c_i}{c_0} \cdot 100\ \% \quad (1)$$

where *RE* is the removal efficiency, as a %, c_0 is the initial concentration of the solution, in mg/L, and c_i is the concentration of sample taken from the solution at time *I,* in mg/L.

The classical filtration equation is presented as Eq. (2) (Ripperger et al., 2012):

$$\frac{dt}{dV} = \frac{\mu \alpha_{av} c}{A^2 \Delta P} V + \frac{\mu R_m}{A \Delta P} \quad (2)$$

where t is the filtration time, measures in s, V is the volume of collected filtrate, in m^3, μ is the viscosity of the filtrate, in Pa·s, α_{av} is the average specific cake resistance, in m/kg, c is the filtration concentration, in $kg_{solids}/m^3_{filtrate}$, A is the filtration area, in m^2, ΔP is the pressure drop over the filter cake, in Pa, and R_m is the resistance of the filter media, expressed in 1/m. By plotting t/V versus V, the average specific cake resistance α_{av} can be calculated from the slope as follows:

$$\alpha_{av} = \frac{2A^2 \Delta P}{\mu c} \cdot a \quad (3)$$

where a is the slope, s/m^6.

The filtration concentration, c, refers to the mass of solids per unit of filtrate volume and can be calculated from Eq. (4) (Rushton et al., 2000):

$$c = \frac{c_w \rho_L}{1 - c_w x} \quad (4)$$

where c_w is the concentration of solid matter in the slurry, -, ρ_L is the density of the liquid, in kg/m^3, and x is the moisture ratio, -. Both c_w and x can be determined through the mass of filtered slurry and masses of wet and dry cake from Eqs. (5) and (6) respectively (Svarovsky, 2000):

$$c_w = \frac{m_{d.s.}}{m_{sl}} \quad (5)$$

$$x = \frac{m_{w.c.}}{m_{d.s.}} \quad (6)$$

where m_{sl} is the mass of the slurry, in kg, $m_{d.s.}$ is the mass of the dry cake, in kg, and $m_{w.c.}$ is the mass of wet cake, in kg.

Another reported parameter, the porosity of filter cake, ε, as a %, can be calculated from Eq. (7):

$$\varepsilon = \frac{\rho_s(x-1)}{\rho_L+\rho_s(x-1)} \quad (7)$$

where ρ_s is the density of the solids, in kg/m^3, which was determined by standard pycnometer measurements.

The cake compressibility index, n, is dimensionless, and expresses the influence of the applied filtration pressure on the average cake resistance, α, m/kg, and is determined according to Eq. (8) (Ripperger et al., 2012):

$$\alpha = \alpha_0 \left(\frac{p_S}{p_0}\right)^n \quad (8)$$

where α_0 is the resistance, m/kg, at a standard pressure drop p_0, Pa, p_S is the compressive stress, Pa.

4. Results and discussion

4.1. Summary of the results of the electrochemical water treatment

Before studying the filtration behaviour of slurry formed during the EC-treatment, some laboratory results of electrochemical tests have been summarized in this section. During the electrochemical treatment of mining waters, the removal of sulfate, nitrate and ammonium were monitored. The final pH values of treated solutions were around 12 for Fe anodes and 10.5 for Al anodes, regardless of the initial pH. The main results obtained for sulfate and nitrate removal using the 1 L reactor are presented in Figs. 3 and 4 respectively.

Fig. 3 summarizes the influence of the electrode material and the initial pH of the solution on the sulfate removal. The application of inert electrodes was not efficient and the results from EC-tests with Fe and Al anodes are only reported. As illustrated in Fig. 3, the removal of sulfate varied from 5 to 97%, depending on the operational conditions.

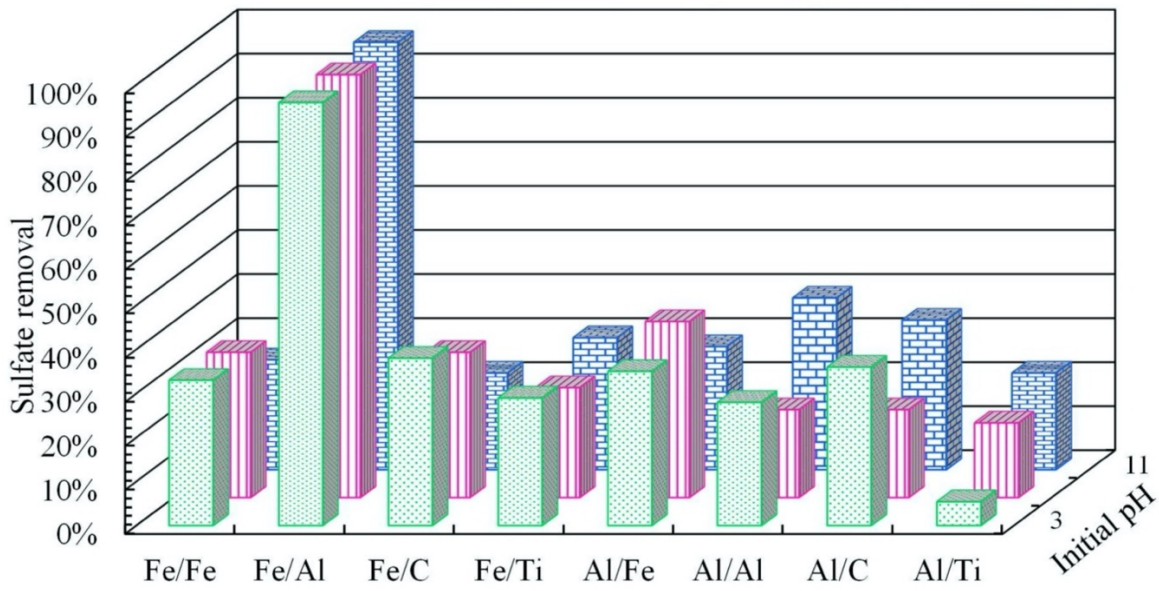

Fig. 3. Effect of electrode material and initial pH on sulfate removal during the electrocoagulation treatment of synthetic mining waters (initial sulfate concentration was 1000 mg/L). The volume of reactor was 1 L.

When Fe anodes were used, the initial pH had no significant influence on the sulfate removal and mostly affected the speciation of species formed during the first hour of treatment. The highest removal of sulfate was obtained using the Fe/Al pair and took place after 2 hours of the treatment. Thus, it can be concluded that the simultaneous presence of iron and aluminium species □avoured the elimination of contaminants. This might be due to a more sufficient generation of solid species (iron and aluminium hydroxides) that were able to adsorb higher amount of sulfate (del Ángel et al., 2014; Kolics et al., 1998; Nariyan et al., 2018). In addition, a moderate (less than 40%) removal of sulfate was achieved using Al anodes. In this case, the highest removal was reported when an Al/Al pair was used at an initial pH of 11. The results obtained with the Al/Al pair are in agreement with the sulfate removal efficiencies in studied ranges of the parameters reported by Nariyan et al. (2018).

Fig. 4. Provides information on the changes in nitrate removal in relation to various electrode combinations and three different initial pH levels of the solution. As can be seen in Fig. 4, during electrocoagulation, the almost complete removal of nitrate was observed after 30 min using an Al/Fe pair at pH 3 or an Fe/Al pair at pH 11. However, when Al/Al and Fe/Fe pairs are used, the pH is not a primary parameter affecting the nitrate removal (Lacasa et al., 2011b). On the other hand, the application of Ti-coated anodes (Ti/C and Ti/Ti pairs) leads to an increase in nitrate concentration. The above-mentioned results can be explained through the nitrate removal mechanisms. When Fe and Al were used as anode materials, the main process was probably the electroreduction of nitrate from nitrites to ammonia and to nitrogen gas (Emamjomeh and Sivakumar, 2009b; Koparal and Ogutveren, 2002). The adsorption of nitrate onto solid species, which was reported by Lacasa et al. (2011b), might be also partially involved in the treatment. In the case of a Ti-anode application, the electrooxidation of ammonium ions to nitrites and further nitrates took place and resulted in an increased concentration of nitrate ions (Siddharth et al., 2018).

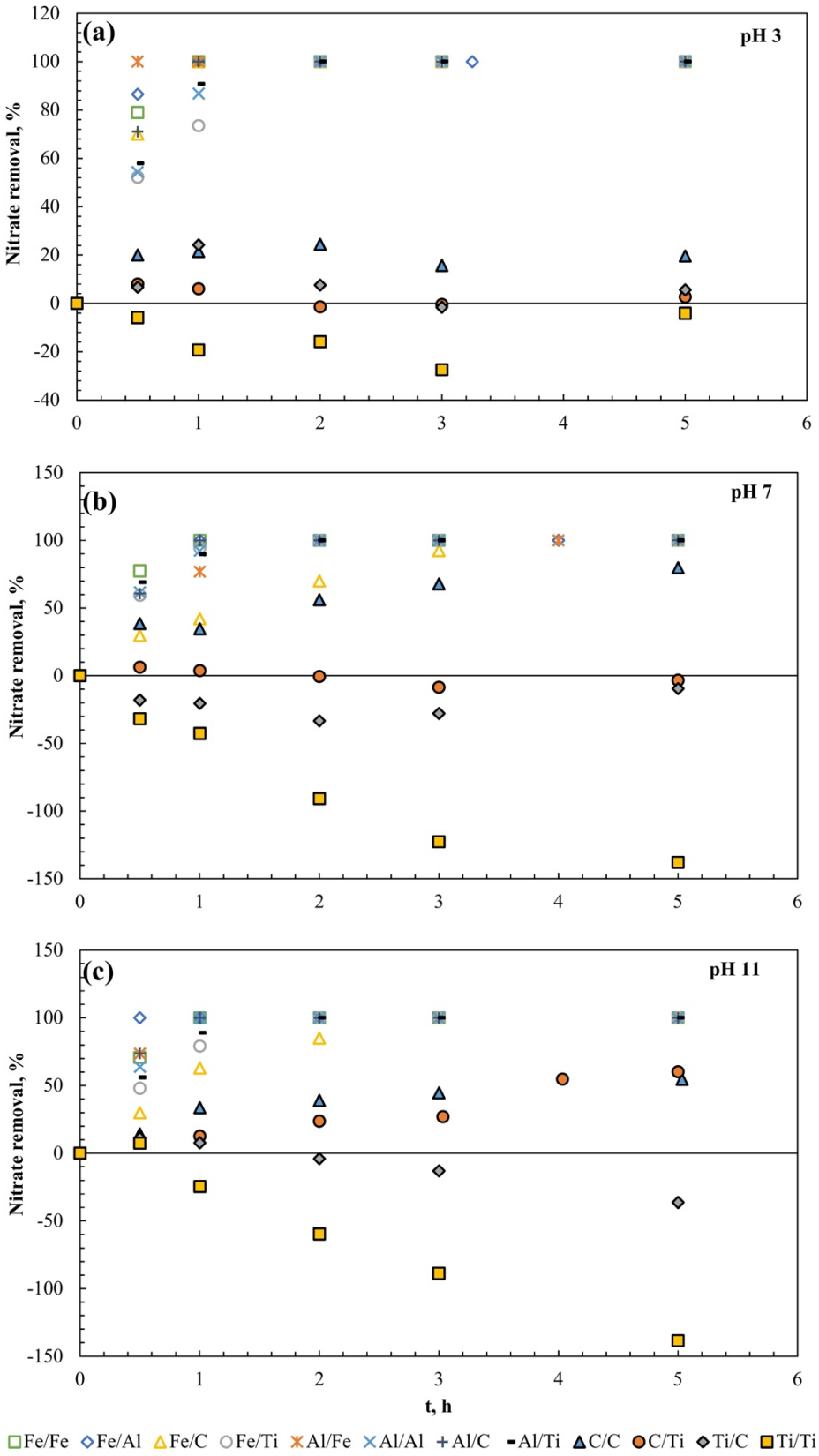

Fig. 4. Effect of electrode material and initial pH on final nitrate concentration during the electrocoagulation treatment of synthetic mining waters (initial nitrate concentration was 10 mg/L). The volume of the reactor was 1 L.

To briefly summarize the results excluded from Figs. 3 and 4, it can be noted that the electrochemical treatment using inert electrode materials, C/C, C/Ti, Ti/Ti and Ti/C, showed poor efficiency in general, and the results of those experiments are therefore not presented in detail. The highest removal of sulfate, 15%, and nitrate, 80%, was achieved with a C/C pair at a pH of 7. However, up to 95% of ammonium was efficiently eliminated by a Ti/C pair at a pH of 3 and 7, and 78% at a pH of 11. A Ti/Ti pair of electrodes enabled the removal of over 95% of ammonium, regardless of the pH, which might be due to the above-mentioned electrooxidation removal of ammonium.

Due to the most efficient treatment of mining waters by EC observed with Fe/Fe, Al/Al and Fe/Al combinations, these pairs were used during the tests in the 70 L reactor. In this work, the current density was used as a scale up parameter. The performance of the electrocoagulation in treatment of synthetic mining water in 1 L and 70 L reactors and in treatment of real mining water in 70 L reactor is summarized in Table III. Regarding the treatment of the synthetic solution, it can be seen in Table III that the removal of contaminants was not as efficient in the 70 L reactor as it was in the 1 L reactor. An increase in the reactor volume from 1 L to 70 L resulted in a decrease in the sulfate removal by 67%, 54% and 9% with Fe/Fe, Al/Al and Fe/Al pairs, respectively. Nitrate was completely removed by using both reactor types. However, the treatment time required for the removal of harmful contaminants increased from 30 min to 5 hours for nitrate and from 2 hours to 5 hours for sulfate. As the current density was chosen as the scale up parameter, the electrode consumption per liter of treated water decreased in the upscaled reactor set-up. This resulted in a lower generation of solids, hence, increasing the treatment time for nitrate removal. The significant decrease in the sulfate removal can be explained by an insufficient amount of hydroxides formed to facilitate the adsorption of sulfate.

When operating the 1 L reactor, the solids generation rate was 3.2 kg/(m^3h) with iron electrodes and 1.9 kg/(m^3h) with aluminium electrodes. When operating the 70 L reactor, the amounts of solids formed were 0.86 kg/(m^3h) and 0.56 kg/(m^3h) for Fe/Fe and Al/Al pairs, respectively. The solid generation rate increased up to 1.1 kg/(m^3h) during the EC-treatment with combined aluminium cathodes and iron anodes. In the case of nitrate and sulfate removal, the mass of solids released per treated volume per hour can be suggested as one of the scale-up parameters for EC.

Comparing the treatment of synthetic and real mining waters (70L reactor), it can be seen in Table III that the efficiency of removal of nitrate from the real mining water was less than half of that obtained for the synthetic solution. The observed decrease in the process performance may be due to the competition between nitrate and co-existing ions (as listed in Table I). However, efficiencies of sulfate removal from both synthetic and real waters with iron electrodes (in 70 L reactor) were comparable, as well as those achieved in EC with aluminium electrodes. As reported by Mamelkina et al. (2019), presence of other ionic species (metal cations) may have a positive effect on removal of sulfate, which might be due to possible initiation of co-precipitation reactions. The achieved removal efficiencies for the presented metals can be found in supplementary materials (Table S-1).

Table III. Comparison of removal efficiencies obtained with 1L and 70L reactors. The initial pH was 3, the current density was 17 mA/cm^2 in all experiments. Superscripts A and B refer to the treatment of synthetic and real mining waters, respectively.

Removal efficiency, %	Electrode material							
	Fe/Fe			Al/Al			Fe/Al	
	1 L^A	70 L^A	70L^B	1 L^A	70 L^A	70L^B	1 L^A	70 L^A
NO_3^-	100	100	38	100	100	46	100	100
SO_4^{2-}	33	11	10	28	13	30	96	87
NH_4^+	–	–	–	2	–	–	5	9
pH_{final}	11.3	10.8	10.3	10.2	8.8	9.0	11.4	11.5

The high final pH (Table III) indicates the high concentration of OH^- ions in the solution. In the case of iron electrodes, the formed Fe (II) ions bound less OH^- ions and therefore resulted in high final pH values. Aluminium electrodes produced Al (III) ions, which bound more OH^- ions compared to Fe (II) and resulted in lower final pH values (Vepsäläinen, 2012). The Fe/Al pair produced the highest pH values, which might be associated to the nature of the formed solids.

4.2. Characterization of solids

The electrocoagulation experiments were performed by using iron and aluminium electrodes. Therefore, iron and aluminium oxides and hydroxides were expected to represent the vast majority of the generated solids. Along with the (hydr)oxides of Fe and Al, various metals were expected to be present in the slurries produced in the treatment of real mining water. In this study, comprehensive analysis of solids was performed only for the sludge of synthetic origin.

The results of the XRD analysis presented in Fig. 5 show that Fe/Fe solids had narrow and sharp peaks of high intensity, which indicates that crystalline phases were formed. Magnetite was the only species recognized explicitly (Fig. 5a), but also hematite or sodium chloride formed during the EC from the corresponding elements were present in small amounts. The analyses of Al/Al and Fe/Al slurries showed broad, less intensive peaks without a strict baseline. This implies that the solid matter is likely to have a poorly crystalline, or for the most part, amorphous structure. Aluminium hydroxides, namely bayerite, boehmite and nordstrandite, were detected in the Al/Al solids (Fig. 5b). However, the Fe/Al matter did not contain the crystalline phases formed in EC with Fe/Fe and Al/Al electrodes. As can be observed in Fig. 5c, the Fe/Al solids were composed from bayerite (similar to Al/Al), goethite and aluminium-substituted goethite. The iron hydroxides prevailed over the aluminium ones due to higher release of iron cations from the iron anodes, compared to the release of aluminium species from the aluminium cathode. Similar results of an XRD analysis of electrode by-products were obtained in studies by Gomez et al. (2007) and Wu et al. (2019).

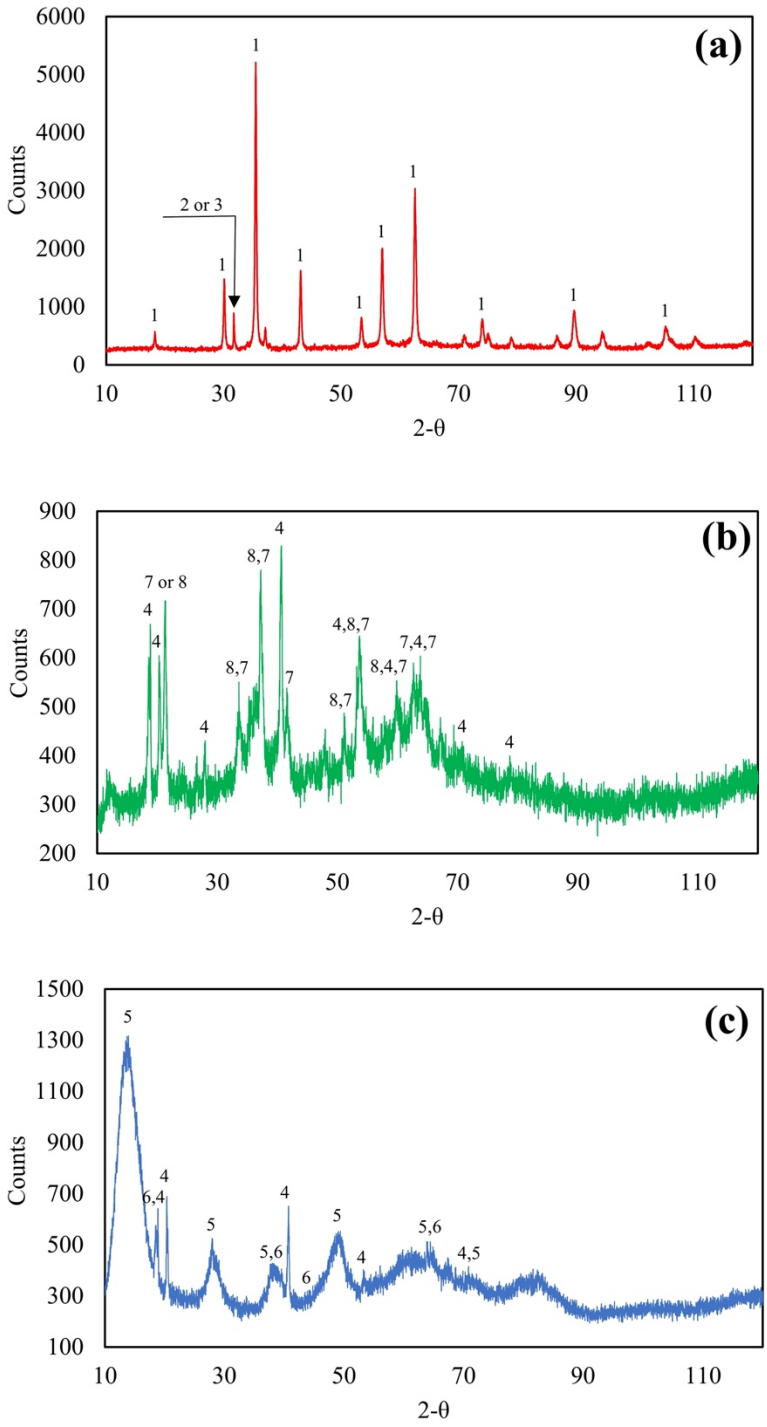

Fig. 5. XRD diffractograms of solids present in (a) Fe/Fe, (b) Al/Al and (c) Fe/Al slurries. Peaks: magnetite, Fe_3O_4: 1, hematite, Fe_2O_3: 2, sodium chloride, NaCl: 3, bayerite, α-$Al(OH)_3$: 4, boehmite, γ-AlO(OH): 5, nordstrandite, $Al(OH)_3$: 6, aluminium-substitute goethite, $(Fe_{0.83}Al_{0.17})O(OH)$: 7, goethite, FeO(OH): 8.

The SEM images of the solid matter in the Fe/Fe, Al/Al and Fe/Al slurries (Fig. 6) show that the solids formed irregular-shaped aggregates. The Fe/Fe matter (Fig. 6a,b) consists of very small (mainly below 100 nm), round primary particles and their aggregates. Solids generated during EC with Al/Al electrodes (Fig. 6c,d) were found to have the most intricate structures among the investigated solids, and these solids formed sponge-like amorphous structures. Fig. 6e and Fig. 6f illustrate the Fe/Al matter, the structure of which has features of the two cases discussed above.

As in Fe/Fe solids, some separate particles can be distinguished. However, the particles seem to be attached to each other creating a continuous network, similarly to the amorphous Al/Al solids. Other researchers (Moussavi et al., 2011; Sandoval et al., 2014; Wu et al., 2019) have reported the presence of amorphous flocs of aluminium and iron hydroxides and their mixtures. However, particles observed in those studies fall into a larger size category of several micrometers. An amorphous structure favours the removal of harmful contaminants because of the large surface area resulting in a high adsorption capacity (Gomez et al., 2007).

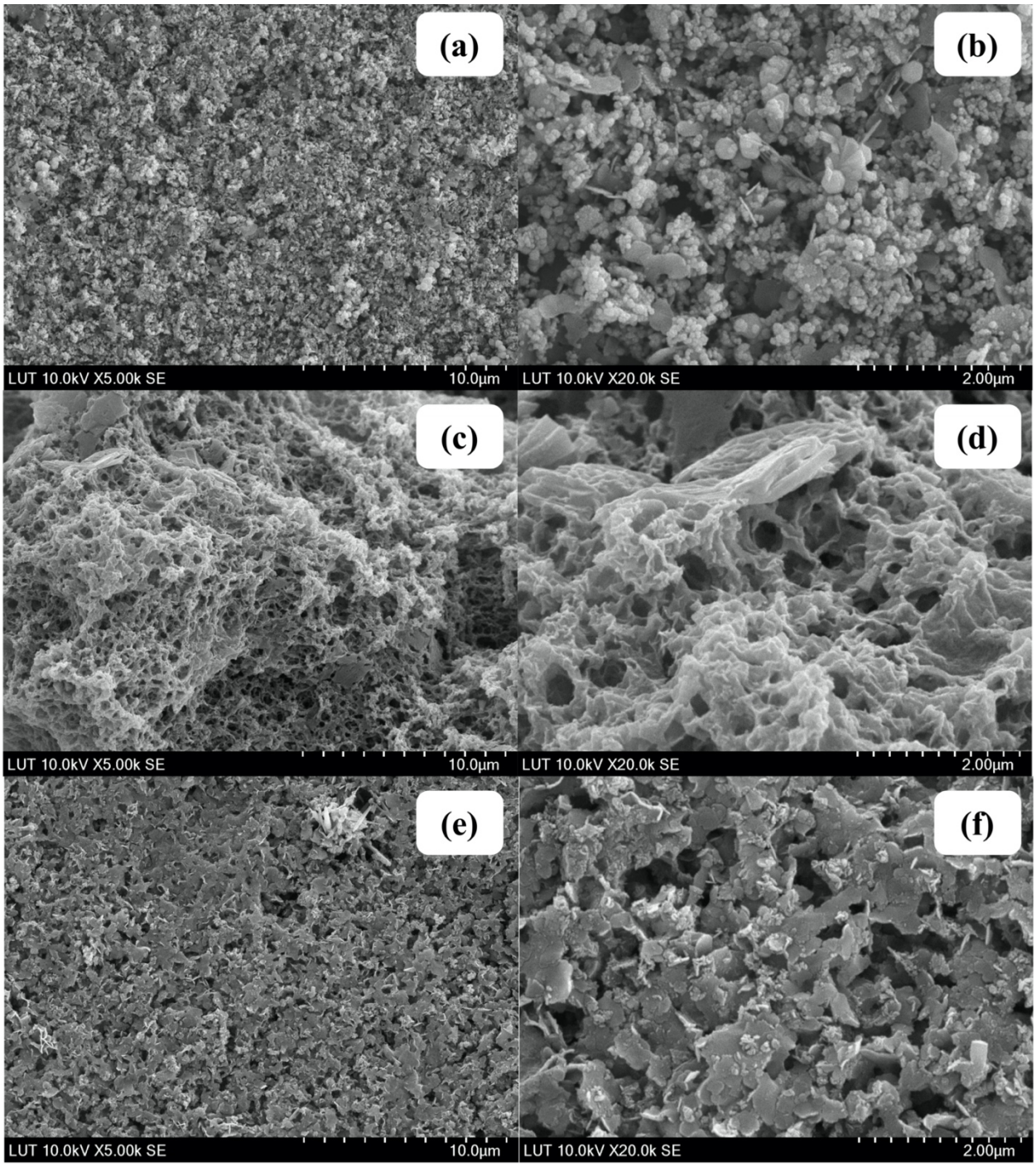

Fig. 6. SEM images of the solids formed by electrocoagulation: Fe/Fe (a, b), Al/Al (c, d) and Fe/Al (e, f).

Fig. 7 shows the number-based (Fig. 7a,c,e) and volume-based (Fig. 7b,d,f) particle size distributions (PSDs) of the slurries obtained during the EC experiments. As the electrocoagulated solids consisted largely of aggregates, it should be pointed out that the presented PSDs are unable to illustrate the size distribution of individual particles. Intensive stirring and ultrasound were applied to break the aggregates into constituent particles in the sample dispersing unit of the particle size analyser, but no changes were observed in the PSD, which apparently indicates a tight binding between the aggregates. As seen in Fig. 7c-f, the size of the Al-based particles tends to increase with time. On the other hand, for the Fe/Fe sludge (Fig. 7a, b) the trend is the opposite. The Fe/Fe solids are the only ones consisting of clearly observable primary particles, whereas the solid formations in Al/Al and Fe/Al slurries were completely different. In these cases, generation of new solid particles from the consumable electrodes seems to proceed together with the formation of agglomerates that results in peak broadening. Among the EC solids, Al/Al agglomerates were the largest. Iron-containing solids had the narrowest and the least time-dependent size distribution, and also the volume-based distributions reflected the same trend.

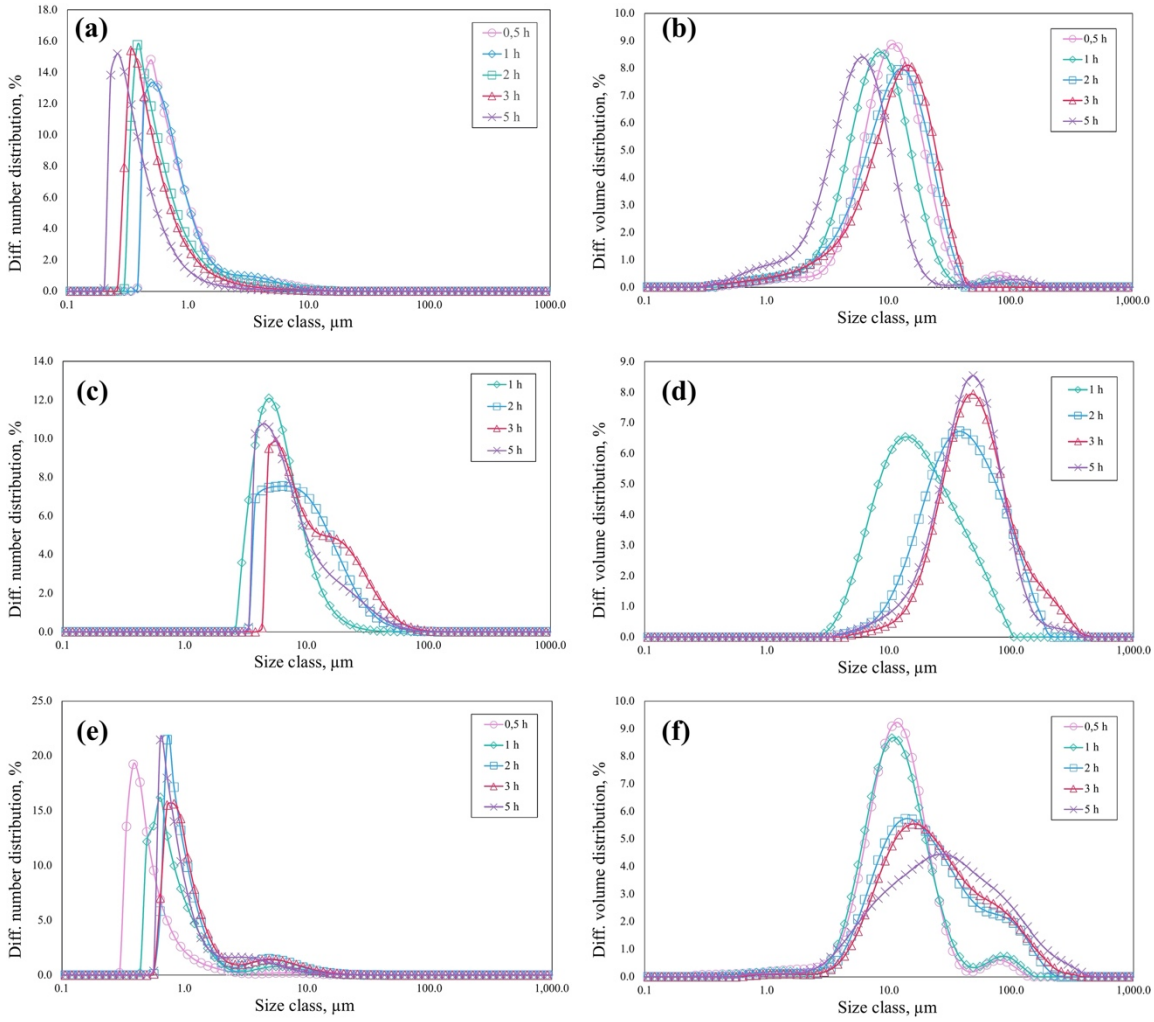

Fig. 7. Particle size distributions of solids presented in Fe/Fe (a, b), Al/Al (c, d) and Fe/Al (e, f) slurries (a, c and e represent number-based PSD; b, d and f depict volume-based PSD).

Comparing the number- and volume-based distributions, it can be seen that primary particles dominate in the Fe/Fe sludge as the most frequently occurring sizes in the number-based (Fig. 7a) and volume-based (Fig. 7b) PSDs were lower than 1 and around 10 μm respectively. The predominant particle size in the Al/Al PSD (Figs. 7c,d) is about 10 times larger, compared to that of the Fe/Fe species, which indicates that these are large agglomerates in the Al/Al sludge, where practically no primary particles were observed, referring to Fig. 5 above. A combination of these cases is observed in the PSD of Fe/Al solids: primary particles were predominant in the number distribution (Fig. 7e) but aggregates mainly determined the volumetric distribution (Fig. 7d).

4.3. Characterization of the slurries

The main characteristics of the electrochemically generated sludges are presented in Table IV, where the term "concentration" stands for settling and decantation performed to increase the suspended solid content prior to filtration. Both EC-treated and 48-hours concentrated slurries had densities which were only slightly higher than pure water (all measured at 20° C), although the true densities of the dry solids were relatively close to conventional values which are 5150 kg/m^3 for pure magnetite ("Magnetite mineral data", 2020) and 2420 kg/m^3 for pure aluminium hydroxide ("PubChem" open database, 2020).

Table IV. Characteristics of the electrochemically generated slurries and solid matter. Superscripts *A* and *B* refer to the characteristics of sludge obtained by the EC treatment of synthetic and real mining waters, respectively.

Characteristic	Type of sludge				
	Fe/Fe^A	Fe/Fe^B	Al/Al^A	Al/Al^B	Fe/Al^A
Amount of released electrode material, after 5 h of EC, g/L	4.3	N/a	2.8	N/a	5.5
Density of sludge after 5 h of EC, kg/m^3	1,019	1,012	1,004	1,002	1,002
Density of sludge after 48 h of concentration, kg/m^3	1,026	1,017	1,011	1,007	1,009
Solids content of concentrated sludge, wt%	4.26	4.01	2.09	1.23	2.05
True density of solids, kg/m^3	4,316	4,779	2,696	3,150	3,146

4.4. Pressure filtration

The main results of the pressure filtration experiments are reported in Table V. Hereinafter, the values presented in the text refer to the case of synthetic mining water. However, as can be seen in Table V, the cakes obtained in filtration of slurries produced during the EC of real water demonstrated similar characteristics and filtration properties. Representative examples of the obtained filter cakes are shown in Fig. 8.

The filter cakes were found to have porosity ε values in the range of 90–97%. The highest porosities were observed for Al/Al cakes, ($\varepsilon > 96\%$ in all cases), while cakes formed from Fe/Fe sludge had the lowest porosities (90–94%). The weight-based moisture content (MC) was within the range of 90–92% in Al/Al cakes. The moisture contents of Fe/Al and Fe/Fe cakes were lower, 77–83% and 68–77%, respectively. The high moisture contents and porosities result from the complex pore structure of the cake formed from coagulated solids that have a high amorphous content and a high-water retention capacity. According to the literature (Stickland, 2015), chemically coagulated solids produced in water treatment can form an interconnected network, i.e. reach the gel point, even at concentrations below 1 vol%.

The average specific cake resistances α_{av} of filter cakes were relatively high, which is typical of cakes formed from compressive suspensions (Wetterling et al., 2014). The Fe/Fe cakes had the lowest average specific cake resistances, whereas the average specific resistances determined for Al/Al and Fe/Al cakes were by about an order of magnitude higher than those for the Fe/Fe cakes.

The correlation between the applied pressure difference and other filtration characteristics was as expected: shorter filtration times and a lower MC can be achieved by applying higher filtration pressure. However, the increase in the operating pressure resulted in higher cake resistance, i.e. the cakes were compressible, which is undesirable, because the filtration capacity does not increase linearly with the applied pressure. The cake compressibility indices n indicated that iron-containing solid matter (Fe/Fe and Fe/Al sludge) formed mainly moderately compressible filter cakes, and the cakes composed of Al/Al solids were less compressible. However, the compressibility indices should be regarded as approximate values only due to the limited number of data points used for their determination, and the variations in the n determined for the same sludge using different slurry volumes are likely to reflect the determination inaccuracy, but may also indicate a different interaction between the sludge and the filter medium, such as formation of a poorly permeable skin layer (see Mattsson et al. 2012) at the surface of the filter medium.

Table V. The effect of the type of sludge, volume of the filtered sample and the pressure difference on filter cake characteristics such as porosity, ε, moisture content, *MC*, compressibility index, *n*, and average specific cake resistance, α_{av}, and filtration time.

Iron electrodes						Aluminium electrodes					Iron anodes and Aluminium cathodes				
Slurries obtained during EC of synthetic mining water															
Δp [bar]	*ε* [%]	*MC* [%]	*n* [-]	α_{av} [m/kg]	*time* [min]	*ε* [%]	*MC* [%]	*n* [-]	α_{av} [m/kg]	*time* [min]	*ε* [%]	*MC* [%]	*n* [-]	α_{av} [m/kg]	*time* [min]
V_{sl} = 300 mL															
2	92.91	75.18		$2.172 \cdot 10^{12}$	28.78	96.44	90.92		$2.126 \cdot 10^{13}$	127.01	93.30	81.55		$1.909 \cdot 10^{13}$	129.30
4	92.23	73.30	0.75	$3.506 \cdot 10^{12}$	24.87	96.34	90.68	0.40	$3.365 \cdot 10^{13}$	98.82	93.91	83.02	0.55	$3.317 \cdot 10^{13}$	107.42
6	90.52	68.82		$4.999 \cdot 10^{12}$	22.58	96.59	91.30		$3.178 \cdot 10^{13}$	60.24	91.67	77.75		$3.373 \cdot 10^{13}$	70.71
V_{sl} = 200 mL															
2	93.51	76.92		$2.178 \cdot 10^{12}$	12.22	96.51	91.10		$2.262 \cdot 10^{13}$	55.31	93.58	82.23		$1.573 \cdot 10^{13}$	45.97
4	93.29	76.27	0.74	$3.439 \cdot 10^{12}$	10.42	96.62	91.37	0.34	$3.087 \cdot 10^{13}$	38.10	93.84	82.87	0.85	$3.123 \cdot 10^{13}$	45.30
6	91.71	71.90		$4.982 \cdot 10^{12}$	9.92	96.81	91.83		$3.256 \cdot 10^{13}$	27.38	93.55	82.16		$3.933 \cdot 10^{13}$	37.65
V_{sl} = 100 mL															
2	92.64	74.43		$2.317 \cdot 10^{12}$	2.82	96.52	91.13		$2.074 \cdot 10^{13}$	12.45	93.43	81.87		$1.384 \cdot 10^{13}$	10.20
4	91.91	72.42	0.73	$3.818 \cdot 10^{12}$	2.40	96.63	91.39	0.57	$3.356 \cdot 10^{13}$	9.80	92.69	80.10	0.96	$3.278 \cdot 10^{13}$	9.60
6	91.80	72.14		$5.184 \cdot 10^{12}$	1.98	96.29	90.57		$3.794 \cdot 10^{13}$	7.73	93.61	82.30		$3.848 \cdot 10^{13}$	7.93
Slurries obtained during EC of real mining water															
V_{sl} = 200 mL															
2	93.90	76.20		$2.506 \cdot 10^{12}$	30.24	98.30	94.70		$4.308 \cdot 10^{12}$	59.45					
4	93.80	76.40	0.18	$3.696 \cdot 10^{12}$	22.65	98.10	94.20	0.25	$8.070 \cdot 10^{12}$	40.87			N/a		
6	92.20	71.20		$4.999 \cdot 10^{12}$	21.12	97.90	93.70		$1.171 \cdot 10^{13}$	30.01					

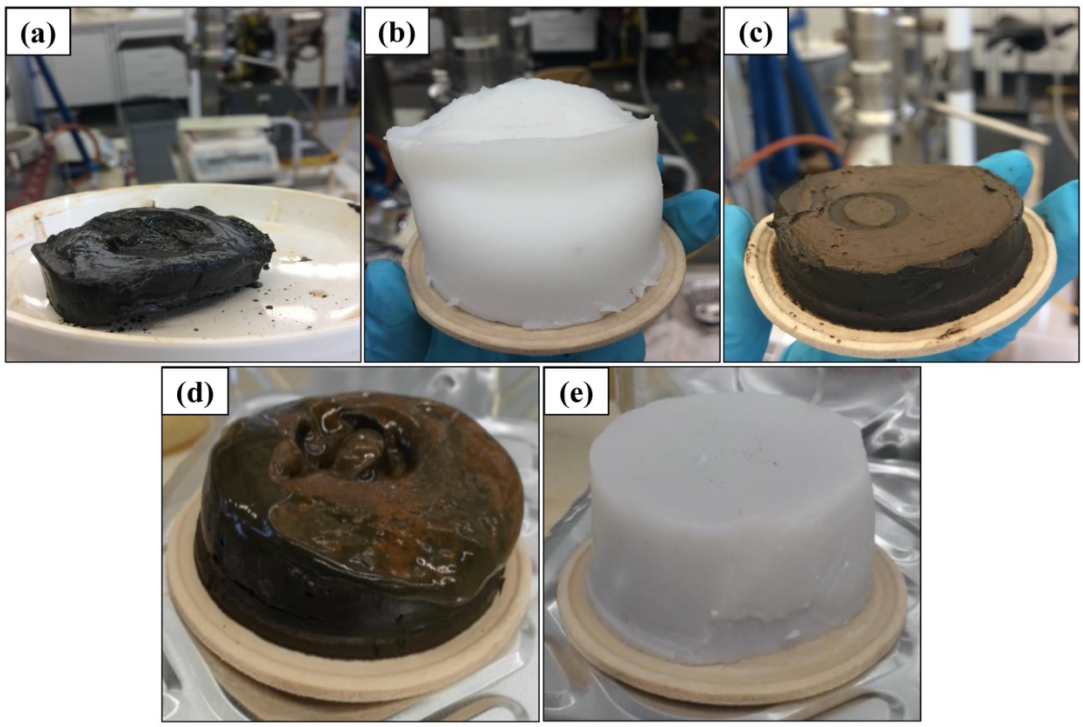

Fig. 8. Cakes formed by the pressure filtration of synthetic[A] and real[B] mining water-originated sludges: Fe/Fe[A] (a), Al/Al[A] (b), Al/Fe[A] (c), Fe/Fe[B] (d), Al/Al[B] (e) at a pressure difference of 6 bar. The applied batch volumes were 100 mL (a and b) and 200 mL (c, d and e).

The small size of the primary particles as well as the correspondingly large specific surface area (SSA) of their aggregates may partly explain the high observed specific cake resistances, high porosities and moisture contents, as demonstrated by Wakeman (2007). The larger the SSA, the higher the ability of solids to attract and retain molecules, such as water. Moreover, the agglomerates exhibited a highly porous structure, especially in the case of Al/Al solids that resembled a sponge-like material. Thus, the highly porous and largely amorphous solid aggregates may be the main reason for the high-water retention. According to the related literature (Shin and Lee, 2006; Wu et al., 2019), water can be (1) entrapped between the primary solids in the moment of floc formation, (2) attached to the developed SSA of the aggregates or flocs, and (3) retained in a porous space between the flocs. On the other hand, Tsang and Vesilind (1990) identified four types of moisture in dewatered wastewater sludge cakes: (1) free water entrapped in voids, (2) interstitial water retained by capillary forces, (3) surface water (by adhesion or adsorption), and (4) chemically bound water, among which the former two dominate.

While the porosities of all cakes were close to each other, the MC of the cakes in descending order were Al/Al > Fe/Al > Fe/Fe. Similar observations were made for chemically coagulated sludges by Monk and Willis (1987) and Thompson and Paulson (1998), who reported that iron-composed sludges tend to dewater faster and further than aluminium ones.

4.5. Pressure filtration with filter aids

The effect of filter aids (FAs) on the pressure filtration performance was studied by only using Fe/Al sludge that had the highest average specific cake resistances without the use of FAs.

According to the results of the body feed FA filtration tests (Table VI), no significant improvement in any of the filtration characteristics was observed when the FAs were applied at concentrations of 25 or 50 wt% (relative to the mass of solids in the sludge). An increase of the FA content in the sludge body feed resulted in a reduction of the moisture content and average specific resistances of the cakes.

Table VI. The effect of the concentration of filter aids on the filtration characteristics. The body-feed filtration of the Fe/Al sludge, batch volume was 200 mL, the initial pH was 11.7, and the filtration pressure was 6 bar.

Filter aid	FA conc. [wt% of sludge solids]	Δp [bar]	α_{av} [m/kg]	Moisture content [wt%]	Filtrate recovery [%]
No FA	-	6	$3.93 \cdot 10^{13}$	82.2	100.0
DE	50	6	$2.94 \cdot 10^{13}$	83.8	78.8
	100	6	$9.48 \cdot 10^{12}$	67.7	87.7
	200	6	$4.13 \cdot 10^{12}$	73.6	81.2
RHA X+100	50	6	$2.47 \cdot 10^{13}$	85.5	78.3
	100	6	$8.18 \cdot 10^{12}$	80.9	82.9
	200	6	$2.11 \cdot 10^{12}$	78.3	73.0
RHA Grade 4	25	6	$3.98 \cdot 10^{13}$	86.9	83.8
	50	6	$3.01 \cdot 10^{13}$	81.1	85.1
	100	6	$9.86 \cdot 10^{12}$	67.2	80.8
	200	6	$4.30 \cdot 10^{12}$	71.9	79.3
DE	200	2	$2.88 \cdot 10^{12}$	77.3	79.2
	200	4	$4.51 \cdot 10^{12}$	72.4	77.4
	200	6	$4.13 \cdot 10^{12}$	73.6	81.2
RHA X+100	200	2	$1.62 \cdot 10^{12}$	79.6	70.0
	200	4	$1.76 \cdot 10^{12}$	76.9	76.9
	200	6	$2.11 \cdot 10^{12}$	78.3	73.0
RHA Grade 4	200	2	$3.69 \cdot 10^{12}$	76.3	69.6
	200	4	$4.27 \cdot 10^{12}$	78.3	70.5
	200	6	$4.30 \cdot 10^{12}$	71.9	79.3

In all the experiments with FAs, the amount of recovered filtrate decreased, compared to the base case (filtration without addition of FAs), due to the increased content of water-retaining solids in the cake. The highest filtrate recovery was achieved with a 100% dosage of diatomaceous earth (DE), followed by 50 and 25% dosages of rice hull ash (RHA) Grade 4 and RHA X+100 (100%). Indeed, DE has the smallest particles, the narrowest PSD and the most regular shape among the used FAs (Kinnarinen et al., 2013), which favours filtration (Carman, 1938; Svarovsky, 2000), whereas X+100 ash is characterized by the largest PSD and a more irregular shape. Even though

the zeta potentials of the FA solids were not measured in this study, it might be anticipated that at the measured sludge pH of 11.7, DE particles would exhibit a low negative charge as reported by Roebuck and Tremblay (2017). At the same time, very fine, non-coagulated particles of metal hydroxides might have slightly positive electrical charges, and once they come into contact with DE, they attach to its negatively charged surface (Carman, 1938).

In general, the moisture content of the filter cakes decreased with an increasing FA concentration. The highest improvements in cake dryness of 20 and 14 percentage points were obtained with RHA Grade 4 (100%) and DE (100%), respectively.

The average specific cake resistance decreased in all the FA body feed experiments, except one experiment using RHA Grade 4 (25%), and the lowest values were achieved at a 200% FA dosage with all filter aids. Among the FAs, DE and RHA Grade 4 reduced the average specific cake resistance by almost one order of magnitude, and RHA X+100 did this by more than one order of magnitude. The effect of the operating pressure on the body-feed filtration behaviour was studied with FA concentrations of 200 wt%. The results (Table VI) show that, in general, increasing the operating pressure increased the average specific cake resistance, which indicates that the EC sludge cakes remained compressible after the addition of filter aids as well.

Possible reasons for the positive effect of filter aids include the reduction of channel tortuosity and increasing the rigidity of the cakes, which improves the filtrate flow and reduces the cake compressibility (Carman, 1938; Kinnarinen et al., 2013).

The main results of the precoat filtration experiments are shown in Fig. 9, where it can be seen that the filtrate recovery was 85–90% in all cases that is slightly higher, compared to body feed mode (Table VI). The highest filtrate recovery in the precoat filtration was achieved with the milled cardboard, although only minor differences between the filter aids were observed. In this case, the moisture content of the filter cakes was not significantly affected by the use of FAs. The average specific cake resistance α_{av} was reduced by all the tested precoat materials, but the reduction was significant only with cardboard (40%) and RHA X+100 (84%).

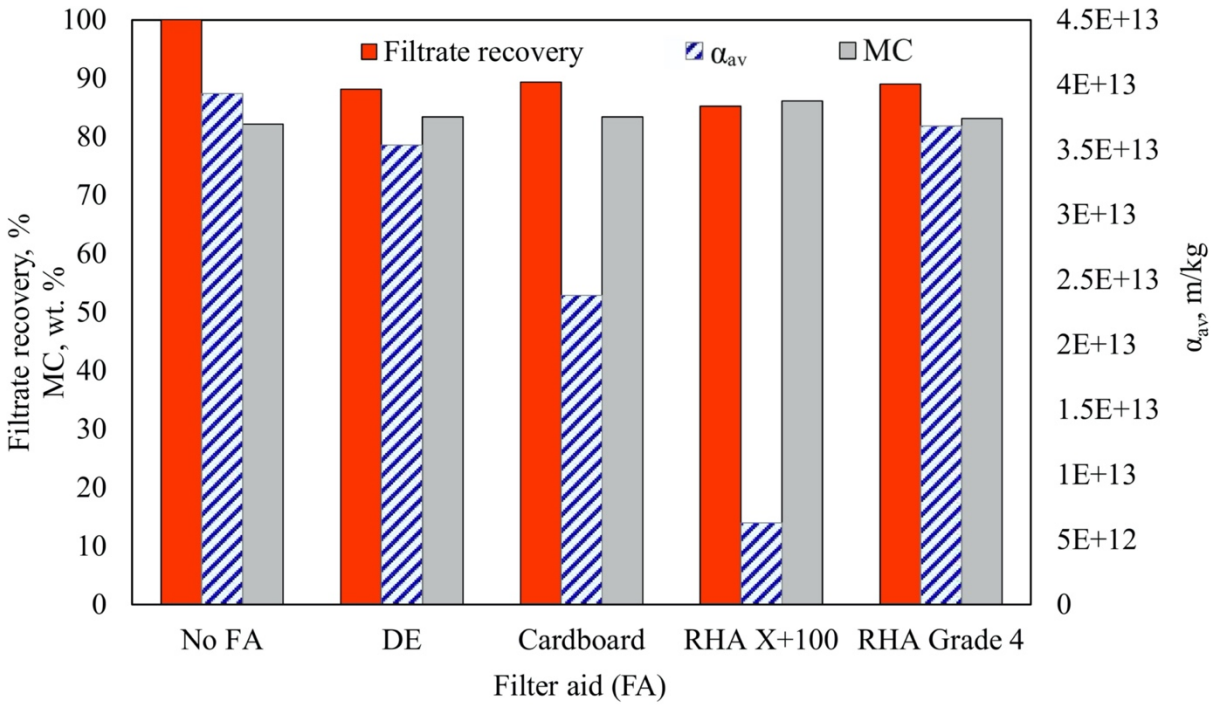

Fig. 9. Filtration of Fe/Al sludge with an FA (100%) precoat. The filtration pressure was 6 bar.

5. Conclusions

The objective of this experimental study was to investigate effects of various variables of electrocoagulation (EC) process from the perspective of solids separation and characterization. The results show that it is possible to achieve the efficient removal of contaminants, and to separate the produced EC sludge using pressure filtration techniques, in spite of the challenges caused by the distinctive properties of the solids.

The ability of EC to remove a particular contaminant is determined among other factors by the used electrodes. Ammonium was better removed with inert (C, Ti) electrodes, whereas the removal of nitrate and sulfate was effective with pairs where at least one anode was made of a consumable material (Fe, Al). This can be explained by the involved removal mechanisms. Solids generated during EC with sacrificial iron electrodes were mainly species of crystalline magnetite, where small primary particles were recognized. The solids generated by Al/Al and Fe/Al electrodes were mainly hydroxides that were found to be largely amorphous, agglomerated and highly porous. No primary particles were detected in the Al/Al solids. These findings are in line with the existing knowledge on sludges generated by chemical coagulation.

In the pressure filtration experiments, the average specific cake resistances and cake moisture contents were high in all cases. The Al-containing solids showed higher cake resistance and moisture contents, probably due to the formation of an interconnected network with a high amorphous content that was capable of holding significant amounts of water while withstanding the applied pressure. The most part of such residual water cannot probably be removed by increasing the pressure difference. However, enhancing the dewatering by using shear, electric methods or microwaves may be useful to some extent.

The use of filter aids improved the filtration in both precoat and body-feed modes due to increased rigidity and reduced channel tortuosity (body-feed) and an apparent reduction of the cake resistance closer to the filter medium (precoat). Although the question of utilization of the filter cakes is beyond the scope of this work, the authors suggest that the cakes could be used, perhaps after modification, to produce adsorbent materials, or to recover the metal content for further use.

Acknowledgements

This work was supported by the EIT Raw Materials [EWT-CYNCOR project, 16391] and the European Union Horizon 2020 program [ITERAMS project, 730480].

REFERENCES

Ben Ali, H.E., Neculita, C.M., Molson, J.W., Maqsoud, A., Zagury, G.J., 2019. Performance of passive systems for mine drainage treatment at low temperature and high salinity: A review. Minerals Engineering 134, 325-344. https://doi.org/10.1016/j.mineng.2019.02.010

Carman, P. C., 1938. The Action of Filter Aids. Industrial & Engineering Chemistry, 30 (10), 1163-1167. https://doi.org/10.1021/ie50346a016¨

Chen, G., 2004. Electrochemical technologies in wastewater treatment. Separation and Purification Technology, 38 (1), 11-41. https://doi.org/10.1016/j.seppur.2003.10.006

Cidu, R., Fanfani, L., 2002. Overview of the environmental geochemistry of mining districts in southwestern Sardinia, Italy. Geochemistry: Exploration, Environment, Analysis, 2, 243-251. https://doi.org/10.1144/1467-787302-028

Cui, H., Li, L.Y., Grace, J.R., 2006. Exploration of remediation of acid rock drainage with clinoptilolite as sorbent in a slurry bubble column for both heavy metal capture and regeneration. Water Research, 40 (18), 3359-3366. https://doi.org/10.1016/j.watres.2006.07.028

Del Ángel, P., Carreño, G., Nava, J.L., Martínez, M.T., Ortiz, J., 214. Removal of arsenic and sulfates from an abandoned mine drainage by electrocoagulation. Influence of hydrodynamic and current density. International Journal of Electrochemical Science, 9, 710-719.

Dolenec, T., Serafimovski, T., Tasev, G., Dobnikar, M., Dolenec, M., Rogan, N., 2007. Major and trace elements in paddy soil contaminated by Pb-Zn mining: a case study of Kocani Field, Macedonia. Environmental Geochemistry and Health, 29 (1), 21-32. https://doi.org/10.1007/s10653-006-9057-x

Duruibe, J. O., Ogwuegbu, M. O. C., Egwurugwu, J. N., 2007. Heavy metal pollution and human biotoxic effects. International Journal of Physical Science, 2 (5), 112-118.

Emamjomeh, M., Sivakumar, M., 2009a. Review of pollutants removed by electrocoagulation and electrocoagulation/ flotation processes. Journal of Environmental Management, 90 (5), 1663-1679. https://doi.org/10.1016/j.jenvman.2008.12.011

Emamjomeh, M., Sivakumar, M., 2009b. Denitrification using a monopolar electrocoagulation/flotation (ECF) process. Journal of Environmental Management, 91, 516-522. https://doi.org/10.1016/j.jenvman.2009.09.020

Emamjomeh, M.M., Sivakumar, M., Varyani, A.S., 2011. Analysis and the understanding of fluoride removal mechanisms by an electrocoagulation/flotation (ECF) process. Desalination, 275 (1-3), 102-106. https://doi.org/10.1016/j.desal.2011.02.032

Gomes, J.A., Daida, P., Kesmez, M., Weir, M., Moreno, H., Parga, J.R., Cocke, D.L., 2007. Arsenic removal by electrocoagulation using combined Al–Fe electrode system and characterization of products. Journal of Hazardous Materials, 139 (2), pp. 220-231. https://doi.org/10.1016/j.jhazmat.2005.11.108

Harmsen, J., 2013. Industrial process scale-up: a practical innovation guide from idea to commercial implementation. First Edition, 112 pp. Elsevier, Oxford, UK.

Hassani, G., Nasser S., Gharibi, H., 2011. Removal of Cyanide by Electrocoagulation Process. Analytical & Bioanalytical Electrochemistry, 3 (6), 625-634.

Holt, P.K., Barton, G.W., Wark, M., Mitchell, C.A., 2002. A quantitative comparison between chemical dosing and electrocoagulation. Colloids and Surfaces A: Physicochemical and Engineering Aspects, 211 (2-3), 233-248. https://doi.org/10.1016/S0927-7757(02)00285-6

Johnson, D.B., Hallberg, K.B., 2005. Acid mine drainage remediation options: A review. Science of the Total Environment, 338 (1-2), 3-14. https://doi.org/10.1016/j.scitotenv.2004.09.002

Kabdaşlı, I., Arslan-Alaton, I., Ölmez-Hancı, T., Tünay, O., 2012. Electrocoagulation applications for industrial wastewaters: a critical review. Environmental Technology Reviews, 1 (1), 2-45. https://doi.org/10.1080/21622515.2012.715390

Kinnarinen, T., Golmaei, M., Häkkinen A., 2013. Use of Filter Aids to Improve the Filterability of Enzymatically Hydrolyzed Biomass Suspensions. Industrial & Engineering Chemistry Research, 52 (42), 14955-14964. https://doi.org/10.1021/ie4021057

Kolics, A., Polkinghorne, J.C., Wieckowski, A., 1998. Adsorption of sulfate and chloride ions on aluminum. Electrochimica Acta, 43 (18), 2605–2618. https://doi.org/10.1016/S0013-4686(97)10188-8

Koparal, A.S., Ogutveren, U.B., 2002. Removal of nitrate from water by electroreduction and electrocoagulation. Journal of Hazardous Materials, 89 (1), 83-94. https://doi.org/10.1016/S0304-3894(01)00301-6

Lacasa, E., Cañizares, P., Sáez, C., Fernández, F.J., Rodrigo, M.A., 2011a. Electrochemical phosphates removal using iron and aluminium electrodes. Chemical Engineering Journal, 172 (1), 137-143. https://doi.org/10.1016/j.cej.2011.05.080

Lacasa, E., Cañizares, P., Sáez, C., Fernández, F.J., Rodrigo, M.A., 2011b. Removal of nitrates from groundwater by electrocoagulation. Chemical Engineering Journal, 171 (3), 1012-1017. https://doi.org/10.1016/j.cej.2011.04.053

Liu, J., Zhu, G., Wan, P., Ying, Z., Ren, B., Zhang, P., Wang, Z., 2017. Current applications of electrocoagulation in water treatment: a review. Desalination and Water Treatment, 74, 53-70. https://doi.org/10.5004/dwt.2017.20371

Lottermoser, B.G., 2010. Mine Wastes: Characterization, Treatment and Environmental Impacts. Third Edition, 400 pp. Springer, Verlag Berlin Heidelberg, Germany. https://doi.org/10.1007/978-3-642-12419-8

Mamelkina, M.A., Cotillas, S., Lacasa, E., Sáez, C., Tuunila, R., Sillanpää, M., Häkkinen, A., Rodrigo, M.A., 2017. Removal of sulfate from mining waters by electrocoagulation. Separation and Purification Technology, 182, 87-93. https://doi.org/10.1016/j.seppur.2017.03.044

Mamelkina, M.A., Herraiz-Carboné, M., Cotillas, S., Lacasa, E., Sáez, C., Tuunila, R., Sillanpää, M., Häkkinen, A., Rodrigo, M.A., 2020. Treatment of mining wastewater polluted with cyanide by coagulation processes: a mechanistic study. Separation and Purification Technology, 237, 116345. https://doi.org/10.1016/j.seppur.2019.116345

Mamelkina., M., Vasilyev, F., Tuunila, R., Sillanpää, M., Häkkinen, A., 2019. Investigation of the parameters affecting the treatment of mining waters by electrocoagulation. Journal of Water Process Engineering, 32, 1-9. https://doi.org/10.1016/j.jwpe.2019.100929

Mattsson, T., Sedih, M., Theliander, H., 2012. Filtration properties and skin formation of micro-crystalline cellulose. Separation and Purification Technology, 96, 139-146. https://doi.org/10.1016/j.seppur.2012.05.029

Mollah, M.Y.A., Schennach, R., Parga, J.R., Cocke, D.L., 2001. Electrocoagulation (EC)- Science and applications. Journal of Hazardous Materials, 84 (1), 29-41. https://doi.org/10.1016/S0304-3894(01)00176-5

Monk, R.D.G., Willis, J.F., 1987. Designing Water Treatment Facilities. Journal of American Water Works Association, 79 (2), 45-57. https://doi.org/10.1002/j.1551-8833.1987.tb02798.x

Murugananthan, M., Bhaskar Raju, G., Prabhakar, S., 2004. Removal of sulfide, sulfate and sulfite ions by electro coagulation. Journal of Hazardous Materials, 109 (1-3), 37-44. https://doi.org/10.1016/j.jhazmat.2003.12.009

Nariyan, E., Wolkersdorfer, C., Sillanpää, M., 2018. Sulfate removal from acid mine water from the deepest active European mine by precipitation and various electrocoagulation configurations. Journal of Environmental Management, 227, 162-171. https://doi.org/10.1016/j.jenvman.2018.08.095

Ripperger, S., Gösele, W., Alt, C., 2012. Filtration, 1. Fundamentals. Ullmann's Encyclopedia of Industrial Chemistry. https://doi.org/10.1002/14356007.b02_10.pub3

Roebuck, K., Tremblay, A.Y., 2017, Highly permeable twinned alumina nanoparticles for the precoat filtration of fine colloids. Separation and purification Technology, 182, 197-206. https://doi.org/10.1016/j.seppur.2017.03.045

Rushton, A., Ward, A., Holdich, R., 2000. Solid-Liquid Filtration and Separation Technology, Second Edition. Wiley-VCH, Darmstadt, Germany.

Sahu, O., Mazumdar, B., Chaudhari, P.K., 2014. Treatment of wastewater by electrocoagulation: a review. Environmental Science and Pollution Research, 21 (4), 2397-2413. https://doi.org/10.1007/s11356-013-2208-6

Sandoval, M.A., Fuentes, R., Nava, J.L., Rodríguez, I., 2014. Fluoride removal from drinking water by electrocoagulation in a continuous filter press reactor coupled to a flocculator and clarifier. Separation and Purification Technology, 134 (25), 163-170. https://doi.org/10.1016/j.seppur.2014.07.034

Sarmiento, A.M., Nieto, J.M., Olías, M., Cánovas, C.R., 2009. Hydrochemical characteristics and seasonal influence on the pollution by acid mine drainage in the Odiel river basin (SW Spain). Applied Geochemistry, 24 (4), 697-714. https://doi.org/10.1016/j.apgeochem.2008.12.025

Seal, R.R., Hammarstrom, J.M., Johnson, A.N., Piatak, N.M., Wandless, G.A., 2008., Environmental geochemistry of a Kuroko-type massive sulfide deposit at the abandoned Valzinco mine, Virginia, USA. Applied Geochemistry, 23 (2), 320-342. https://doi.org/10.1016/j.apgeochem.2007.10.001

Shin, H.-S., Lee, J.-K., 2006. Performance evaluation of electrocoagulation and dewatering system for reduction of water content in sewage sludge. Korean Journal of Chemical Engineering, 23 (2), 188-193. https://doi.org/10.1007/BF02705714

Siddharth, K., Chan, Y., Wang, L., Shao, M., 2018. Ammonia electro-oxidation reaction: recent development in mechanistic understanding and electrocatalyst design. Current Opinion in Electrochemistry, 9, 151-157. https://doi.org/10.1016/j.coelec.2018.03.011

Simate, G.S., Ndlovu, S., 2014. Acid mine drainage: Challenges and opportunities. Journal of Environmental Chemical Engineering, 2 (3), 1785-1803. https://doi.org/10.1016/j.jece.2014.07.021

Stickland, A., 2015. Compressional rheology: A tool for understanding compressibility effects in sludge dewatering. Water Research, 82, 37-46. https://doi.org/10.1016/j.watres.2015.04.004

Svarovsky, L., 2000. Solid-Liquid Separation. Fourth Edition, 554 p. Butterworth Heinemann, Oxford, UK.

Tarleton, E.S., Wakeman, R.J., 2007. Solid/Liquid Separation. Equipment Selection and Process Design. 464 p. Elsevier Science. https://doi.org/10.1016/B978-1-85617-421-3.X5000-7

Thompson, P.L., Paulson, W.L., 1998. Dewaterability of alum and ferric coagulation sludges. Journal of American Water Works Association, 90 (4), 164-171. https://doi.org/10.1002/j.1551-8833.1998.tb08419.x

Townsend, I., 2003. Mining: Filtration prospects for the iron ore mining industry, Minerals Engineering. Filtration + Separation, 51 (6), 29-32. https://doi.org/10.1016/S0015-1882(14)70225-3

Tsang, K.R., Vesilind, P.A., 1990. Moisture distribution in sludges. Water Science & Technology, 22 (12), 135-142. doi.org/10.2166/wst.1990.0108

Vepsäläinen, M., 2012. Electrocoagulation in the treatment of industrial waters and wastewaters. Thesis for the degree of Doctor of Science (Technology). VTT Science, Espoo, 19, 96.

Wahlström, M., Kaartinen, T., Mäkinen, J., Punkkinen, H., Häkkinen, A., Mamelkina, M., Tuunila, R., Lamberg, P., Sinche Gonzales, M., Sandru, M., Johnsen, H., Andreassen, J., Harðardóttir, V., Franzson, H., Sund, C., Jansson, K., 2017. Water Conscious Mining (WASCIOUS). 168 pp. Nordic Council of Ministers, Rosendahls, Denmark. http://dx.doi.org/10.6027/TN2017-525

Wakeman, R., 2007. The influence of particle properties on filtration. Separation and Purification Technology, 58 (2), 234-241. https://doi.org/10.1016/j.seppur.2007.03.018

Wetterling, J., Mattsson, T., Theliander, H., 2014. Effects of surface structure on the filtration properties of microcrystalline cellulose. Separation and Purification Technology, 136, 1-9. https://doi.org/10.1016/j.seppur.2014.08.031

Wu, M., Hu, Y., Liu, R., Lin, S., Sun, W., Lu, H., 2019. Electrocoagulation method for treatment and reuse of sulphide mineral processing wastewater: Characterization and kinetics. Science of the Total Environment. 696, 134063. https://doi.org/10.1016/j.scitotenv.2019.134063

Younger, P.L., Banwart, S.A., Hedin, R.S., 2002. Mine water; hydrology, pollution, remediation. 442 p. Kluwer Academic Publishers, Dordrecht, Netherlands. https://doi.org/10.1007/978-94-010-0610-1

Zhu, J., Zhao, H., Ni, J., 2007. Fluoride distribution in electrocoagulation defluoridation process. Separation and Purification Technology, 56 (2), 184-191. https://doi.org/10.1016/j.seppur.2007.01.030

Zolotukhin, I.A., 1989. A pilot-scale system for treatment of mine water by electrocoagulation-flotation. Soviet Journal of Water Chemistry and Technology, 2 (11), 147-151.

Web references:

Magnetite Mineral Data [on line], Mineralogy Database [ref. 06.04.2020]. < URL: http://webmineral.com/data/Magnetite.shtml#.W4MwjOgzaUm >.

Pall Corporation, Data Sheet, 2011, [on line], Pall.com [ref. 06.04.2020]. < URL: https://food-beverage.pall.com/content/dam/pall/food-beverage/literature-library/non-gated/FBTEN.pdf >.

PubChem Open Database, U.S. National Library of Medicine, [on line], PubChem [ref. 06.04.2020]. < URL: https://pubchem.ncbi.nlm.nih.gov/compound/Aluminum-hydroxide >.